Probing Poly(*n*-butyl-methacrylate) Latex Film via Diffusion of Hydrophilic and Hydrophobic Dye Molecules

Andrei Veniaminov,† Thomas Eckert, Hans Sillescu, and Eckhard Bartsch*

Institut für Physikalische Chemie Johannes Gutenberg-Universität, Jakob-Welder-Weg 15, Mainz D-55099 Germany

Received November 30, 2002; Revised Manuscript Received April 30, 2003

ABSTRACT: In the study of holographic grating relaxation (forced Rayleigh scattering, FRS) in nascent latex films we examined poly(*n*-butyl methacrylate) films using two complementary diffusing probes: a hydrophobic fulgide, Aberchrome-540, and its hydrophilic salt derivative. In the former case, the grating decay follows a stretched exponential. Data analysis in terms of a two-state diffusion model yields tracer diffusion coefficients in the cores of the latex particles (10^{-16} m^2 s^{-1}) and the hydroplasticized interface meshes that surround them (10^{-13} m^2 s^{-1}). In the case of the hydrophilic tracer several distinct stages of grating decay can be isolated and interpreted as representing the dye diffusion in water (10^{-10} m^2 s^{-1}), in the interfaces (10^{-13} m^2 s^{-1}), in polymer cores (10^{-16} m^2 s^{-1}), and captured by surfactant clusters (10^{-19} m^2 s^{-1}), respectively. The contributions of particular environments depend on tracer hydrophilicity. Therefore, the two dyes employed provide complementary information on different types of spatial domains in mesoscopically heterogeneous latex films.

Introduction

Polymer latex films have become a viable alternative in the coating technology to films cast from polymer solutions, especially as they allow reducing the amount of volatile organic compounds present in commercial products. However, the replacement of organic solvents by water as dispersion medium has introduced questions of product quality (e.g., with respect to water resistance of waterborne coatings) and of the optimization of latex formulations and drying conditions that have led to intense studies of the drying behavior of latex films by a variety of research techniques during the past decades.[1−3] In particular, due to the application of noninvasive methods like small-angle neutron and X-ray scattering,[4−6] nonradiative energy transfer,[7−10] atomic force microscopy,[11−13] and modern electron microscopy techniques[4,14] which analyze the structure and dynamics of drying latex films on molecular or mesoscopic length scales, a model of the mechanism of film formation has been established.[2,4]

According to this model,[4,15] a drying latex film is a heterogeneous material consisting of three compartments: the polymer phase, the water phase, and an interfacial phase composed of surfactants, charged groups, and counterions which separates the latex particles and interstitial water and is often addressed as hydrophilic membrane. The successful transition from a heterogeneous, wet latex film to a homogeneous, dry polymer film then requires that the membranes break up and that polymer chains diffuse through the particle interfaces into neighboring particles over a distance roughly equal to their radius of gyration. A crucial step for the film formation and the product quality is, thus, the breaking up of the interfaces and its dependence on the type of surfactant present and the time dependence of its spatial distribution in the course of drying. These dependencies are, however, still only poorly understood.[16] Furthermore, the controlled modification of the hydrophilic membranes has recently become an attractive option for tailoring the properties of polymer coatings. Therefore, the development or application of techniques, which enable selective monitoring of the property changes of the hydrophilic membranes during drying, is highly desirable. Quite recently, it has been demonstrated[17−22] that the employment of tracer diffusion techniques is an attractive approach in this direction, leading to a rather detailed quantitative description of the drying process. The basic idea is to add a species of small molecules to the dispersion which are targeted to one specific compartment or to a subset of compartments due to their physical properties (e.g., by their hydrophilicity) and allow to study the property changes in the given compartment by monitoring their translational or rotational motion by suitable methods like direct energy transfer,[17] electron paramagnetic resonance[17,19−21] or holographic grating relaxation.[17,18,22]

Recently, we applied the holographic grating relaxation, or forced Rayleigh scattering (FRS), technique to the tracer diffusion in acrylic polymer latex films.[18,22] We studied[22] poly(*n*-butyl methacrylate-*co*-acrylic acid)—P(BMA-*co*-AA)—latex films at the last stages of drying, from 18 to 0% residual water content (the range limited by the natural requirement of transparent samples), by monitoring the decay of the gratings that were photochemically induced in these films as a result of photoisomerization of implemented dye molecules, accompanied by refractive index modulation. A photochromic fulgide dye,[23] Aberchrome-540 (α-2,5-dimethyl-3-furylethylidene(isopropylidene)succinic anhydride), referred to as ACR-540 in this paper, was chosen for (i) its ability to ensure large photoinduced refractive index modulation ($\Delta n = 7.5\ 10^{-4}$ for 1% of dye concentration[24]) and, hence, a strong diffracted signal, (ii) good long-time thermal stability of both the initial and the photoinduced forms, and (iii) photoreversibility, allowing one to probe the same spot of the sample several times. ACR-540 has been used as an FRS probe in several

* Corresponding author. E-mail: Bartsch@uni-mainz.de.
† On leave from S. I. Vavilov Optical Institute, Birzhevaya line 12, St. Petersburg 199034 Russia.

10.1021/ma0258962 CCC: $25.00
Published on Web 06/05/2003

studies.[18,22,25,26] Although some complications in the identification of the photoproducts were reported,[27] diffusional decay of the gratings induced in homogeneous materials (such as amorphous substances above the glass transition) due to phototransformation of ACR-540 is demonstrated by an exponential shape. If any peculiarities of the decay kinetics are discovered, they can, as a rule, be considered as revealing a specific behavior of the environment. In some cases, an additional relatively weak nondiffusional process was found in the initial part of decay curves, which is independent of the grating distance, Λ, and can thus be separated from the essential diffusional part by varying Λ. In the case of the presence of a rotational contribution this could be isolated by its dependence on the polarization of the reconstructing beam.[28,29]

The probe diffusion which can be monitored by measuring the relaxation of the photoinduced modulation of the optical properties of the sample (via the time decay of the diffraction efficiency) exposed rather unusual features in wet latex films: the relaxation rate τ^{-1} did not show the usual q_Λ^2 dependence ($q_\Lambda = 2\pi/\Lambda$ = grating vector; Λ = grating distance) which is characteristic for Fickian diffusion in homogeneous materials. Analyzing the grating relaxation kinetics in terms of an apparent diffusion coefficient defined as $D_{app} = q_\Lambda^{-2}\langle\tau\rangle^{-1}$ with $\langle\tau\rangle$ being the ensemble-averaged relaxation time, we found that D_{app} does not stay independent of the grating distance. Nor does it decrease with Λ, or time, t, as it would be in the case of barrier-impeded diffusion.[30] In our experiments[18,22] D_{app} grows with growing Λ until saturation is attained at large grating distances. On the other hand, probe diffusion in dried latex films is indistinguishable from the Fickian diffusion found in the solvent-cast polymer films of the same material. Spatial heterogeneity of the wet films on length scales comparable with Λ was found to be the origin of the length scale dependence of $D_{app}(\Lambda)$.

The assumption that spatial domains of two types, with substantially different probe mobilities, exist in the film has made it possible to explain the shape of $D_{app}(\Lambda)$ and determine the tracer diffusion coefficients D in both types of domains. Their characteristic sizes were estimated by the root-mean-squared displacements, M, of the tracer molecule between entering and leaving a given domain. The formalism based on a two-state diffusion model[31−33] was applied; its main statements[22] are briefly reviewed in the next subsection.

These findings resulted from a rather unilateral observation of the behavior of wet latex film from the point of view of a *hydrophobic* tracer, preferably situated in polymer domains with less water—the cores of latex particles. A desirable complementary description requires FRS measurements using a similar molecular tracer, but with *hydrophilic* properties, which predominantly stays in the wet regions, thus probing the hydrophilic interfaces between the latex particles and, possibly, the interstitial water phase. In the present work, we describe the study of poly(*n*-butyl methacrylate)—PBMA—latex films with such a hydrophilic diffusing probe and compare the results with those derived from the motion of its hydrophobic counterpart. We find that the grating relaxation dynamics is more complicated in the case of the hydrophilic tracer as the tracer obviously visits more than two different environments. Thus, the analysis of the motion of the hydrophilic tracer offers a more detailed picture of drying latex films.

Two-State Model of Diffusion in Latex Film

The tracer molecules are supposed to have two diffusional states, e.g., in our case diffusion in two types of spatial domains, referred to as "slow" (s) and "fast" (f), with different diffusion coefficients, $D_{s(f)}$. Transition from one state to the other occurs when a molecule crosses a boundary between adjacent domains of different types. The probe molecule resides in a given domain for the average time of $\tau_{s(f)} = M_{s(f)}^2/6D_{s(f)}$, where the root-mean square displacement $M_{s(f)}$ is considered as a characteristic size of the corresponding domain. The behavior of this model system is driven by two coupled diffusion equations with exchange terms[31−33]

$$(\partial/\partial t)P_s(x,t) = D_s(\partial^2/\partial x^2)P_s(x,t) - \tau_s^{-1}P_s(x,t) + \tau_f^{-1}P_f(x,t) \quad (1a)$$

$$(\partial/\partial t)P_f(x,t) = D_f(\partial^2/\partial x^2)P_f(x,t) - \tau_f^{-1}P_f(x,t) + \tau_s^{-1}P_s(x,t) \quad (1b)$$

where $P_{s(f)}$ are probability densities of the tracer molecules in the corresponding domains. In the limit of a weak sinusoidal grating, the intensity of diffracted light directly measured in FRS experiments decays as the squared modulation amplitude that follows a linear combination of two exponentials:

$$I(t) = I(0)(p'_s \exp(-D'_s q^2 t) + p'_f \exp(-D'_f q^2 t))^2 = (A \exp(-t/\tau_1) + B \exp(-t/\tau_2))^2 \quad (2)$$

The effective diffusion constants D'_s, D'_f and the effective volume fractions p'_s, p'_f are connected to the parameters of the two-state model via

$$D'_{s(f)} = \frac{1}{2}\left(D_s + D_f + \frac{1}{q^2}\left(\frac{1}{\tau_s} + \frac{1}{\tau_f}\right) \mp \sqrt{\left(D_f - D_s + \frac{1}{q^2}\left(\frac{1}{\tau_f} - \frac{1}{\tau_s}\right)\right)^2 + \frac{4}{q^4\tau_s\tau_f}}\right) \quad (3a)$$

$$p'_f = \frac{(p_s D_s + p_f D_f - D'_s)}{D'_f - D'_s}, \quad p'_s = 1 - p'_f \quad (3b)$$

where $p_{s(f)}$ is the probability of a given probe molecule to be in "slow" or "fast" domains: $p_s = \tau_s/(\tau_s + \tau_f) = 1 - p_f$. It should be noted that $p_{s(f)}$ are not simply the volume fractions of the respective domains but additionally depend on the tracer solubilities in (or affinities to) them.

Although the theory predicts a biexponential signal decay (eq 2), a proper description of the observed hologram relaxation due to the diffusion of the tracer molecules could only be provided by a commonly used extension of simple exponential decay, a stretched exponential (Kohlrausch−Williams−Watts, KWW) function:

$$I(t) = I(0)(\exp(-(t/\tau)^\beta))^2 = I(0)\exp(-2(t/\tau)^\beta) \quad (4)$$

which implies a continuous distribution of relaxation times in at least one of the domains; the stretching parameter $0 < \beta < 1$ is a measure of the width of the distribution. From the average relaxation time $\langle\tau\rangle = \tau\beta^{-1}\Gamma(\beta^{-1})$, an apparent diffusion coefficient can be

calculated by the usual relation

$$D_{app} = q_{\Lambda}^{-2}\langle\tau\rangle^{-1} \tag{5}$$

This apparent diffusion coefficient shows a characteristic dependence on the grating distance Λ as it represents a spatial average over the tracer diffusion in the two domains with the relative contributions of "slow" or "fast" domains varying with Λ.

This average (apparent) diffusion coefficient can be expressed in terms two state model as[22]

$$D_{app} = \frac{1}{p'_s/D'_s + p'_f/D'_f} \tag{6}$$

Placing eqs 3 into eq 6, thereby accounting for the Λ dependence of D_{app} since $q = 2\pi/\Lambda$, one obtains a fit-function, which allows one to extract the model parameters D_s, D_f, M_s, and M_f by fits of the grating distance dependence of $D_{app}(\Lambda)$ (see ref 22 for a more detailed treatment of the two-state model and the applied fitting procedure).

Experimental Section

Probe Dyes. The hydrophobic dye, ACR-540 (**I**), was synthesized following the recipe given in refs 34 and 35.

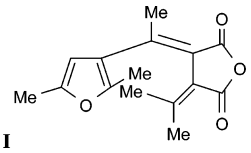

I

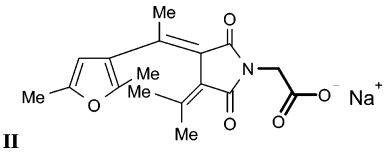

II

To obtain a hydrophilic tracer, ACR-hydr (**II**), with the photochromic properties of ACR-540, the latter was modified as follows.

A solution of ACR-540 in acetone was added to a solution of glycine methyl ester hydrochloride and Na_2CO_3 in water (pH $\approx$ 8). The mixture was stirred at 30 °C for about 24 h. Then the solvent was removed under reduced pressure. After drying the resulting product in a vacuum oven, acetic anhydride and $NaOOCCH_3$ were added, and the mixture heated for 3 h at 80 °C. Then the acetic anhydride was removed and the resulting product was purified by chromatography. The ester was split by adding acetone, water, and Na_2CO_3 and heating (50 °C) the solution during 48 h. After removing the solvents, the product was used for measurements.

The newly synthesized dye (ACR-hydr) retained the chromophore of the parent molecule and its photochromic properties are essentially unchanged. The maximum of the long-wave absorption band of the colored (closed) isomer in dry PBMA is shifted from 490 nm only by a few nanometers into the red, but in water its position is already at 520 nm. A few percent of water present in the films as in the current study influence the spectra only slightly.

Some experiments were performed with phenanthrenequinone (PQ). As this molecule is capable of photochemical bonding to polymer chains, it can serve as a photochemical label for holographic studies of macromolecular diffusion.[29]

Sample Preparation. The photochromic dyes were added (0.5% w/w) to PBMA dispersion (obtained from BASF; average particle radii 107 nm with polydispersity 6.7%, solids content 28%), which was then shaken on a shakeboard during a few days. The films were made by applying a few droplets of the dye-doped latex on the top of a quartz cuvette window and drying at 40 °C, i.e., above both the minimum film forming temperature (27 °C) and the glass transition temperature of the dry polymer (35 °C). After a certain degree of drying, but not before they turned somewhat transparent, the films were covered by another window and placed into the tight metal body of the cuvette. As already noted in refs 4 and 15 water is effectively prevented from further evaporation by this procedure. To flatten the upper surface of the film and ensure optical contact with both windows, the sample (still somewhat soft) was slowly compressed in the holder by screwing the cover. The final thickness of the samples was typically 250−300 μm. Before the measurements, the samples were treated by UV-illumination (wavelength λ = 365 nm) to make them photosensitive to the light of the recording laser (λ = 532 nm). The water content was calculated from the results of weighing the samples before and after FRS measurements (to ensure absence of water loss) and then after complete drying under vacuum (dry weight). For comparative measurements of the dye diffusion in bulk water the hydrophilic tracer was dissolved (0.5% w/w) in bidistilled water and a quartz cuvette with a thickness of 1 mm was filled with the solution. To isolate the effect of the hydrophilic material in the emulsions and that of the specific architecture of latex films, we also examined samples prepared from the pure polymer produced in these polymerizations. For this purpose, the dispersion was coagulated by freezing or water evaporation. The polymer was then purified by repeatedly dissolving it in THF and subsequent precipitation from water. After addition of the dye tracer, the polymer was finally freeze-dried from a benzene solution. Films were prepared by casting from concentrated toluene solution.

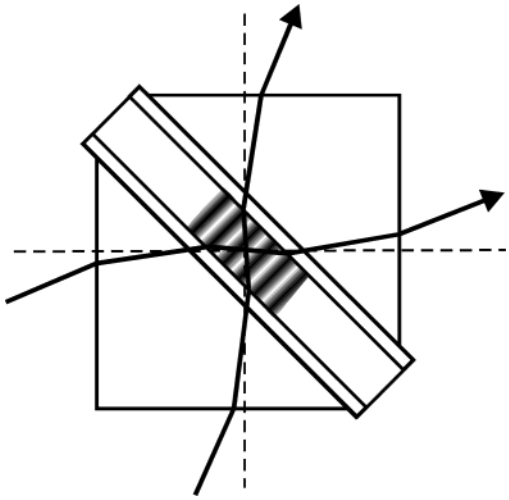

Figure 1. Sample between two prisms, a "cubic" optical scheme that makes the grating periods 0.2−0.3 μm, intermediate between those of transmission- and reflection-type gratings, accessible.

Optical Setup. The experimental setup was in general similar to the one used previously.[22,25,26] Its temporal resolution, limited mainly by the response time of the electromechanical shutters, is now about 20 ms. A continuous wave diode-pumped Nd:YAG laser (Coherent-532-100-cw; second harmonic, λ = 532 nm) was used in this study both for writing the gratings and for their reconstruction. To vary the spatial periods of the gratings, the geometry of the optical experiment was varied. Within the most common transmission scheme (writing beams entering through one side of the sample; interference fringes, hence the grating planes, perpendicular to the surfaces), the grating periods were from 0.4 up to 400 μm, depending on the angle between the beams. In the reflection scheme (writing beams from opposite sides, grating planes almost parallel to the surface) the grating distance was 0.18−0.2 μm. To fill the gap between these two ranges of accessible grating distances, the writing beams were also introduced into the sample, and the diffracted beam obtained from it, through two glass prisms (Figure 1), whose optical contact with the flat glasses covering the polymer film was ensured by a few droplets of glycerol as immersion. By this means, the diffraction gratings with spatial periods of 0.2−0.4 μm were recorded. Such a "cubic" scheme of grating relaxation experiments is convenient for diffusion anisotropy studies as well, since the spatial periods of the gratings

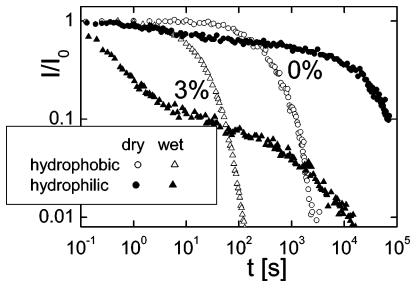

Figure 2. Grating relaxation curves obtained in wet (3% residual water, triangles) and dry (circles) PBMA latex films with hydrophobic (open symbols) and hydrophilic (solid symbols) diffusing probes at 40 °C. Grating period $\Lambda = 1\ \mu$m.

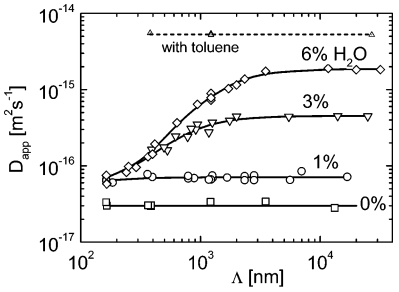

Figure 3. Apparent diffusion coefficient $D_{app} = \langle\tau\rangle^{-1}q_\Lambda^{-2}$ of hydrophobic tracer in PBMA latex films with different concentrations of residual water. On drying the sample, D_{app} changes from a strong grating scale (Λ) dependence at 6% water to a constant value at 1% and below. The data for 2% and 4% water lying between those for 1% and 3% and 3% and 6%, respectively, are not shown. For comparison: the tracer diffusion coefficient stays independent of the spatial scale in the solvent-cast PBMA film plasticized by residual toluene (upper line). The solid lines correspond to fits with the two-state model using eq 6.

recorded parallel and perpendicular to the surfaces of the sample can be made equal, unlike the usual "open surface" geometry. The diameter of the gratings (laser spot size) with $\Lambda < 20\ \mu$m was approximately 1 mm; for larger periods the diameter was increased up to about 8 mm for $\Lambda = 0.4$ mm. The measurements as well as the sample preparation were performed at 40 °C.

Results and Discussion

The results obtained for the diffusion of the hydrophobic tracer ACR-540 in film forming PBMA dispersions were—except for some subtle, but significant quantitative differences—quite similar to the observations made previously[22] in a study of ACR-540 diffusion in latex films of PMBA copolymerized with 1% (w/w) acrylic acid (PBMA-*co*-AA). Thus, we will first interpret the new data within the frame of the two-state model and then discuss the differences between the two materials. Thereafter, we will present the tracer diffusion data obtained with a hydrophilic probe in PBMA and compare them with the observations made with the hydrophobic probe.

Hydrophobic Probe. The decay curves in FRS experiments with ACR-540 (open symbols in Figure 2) were found to be stretched exponential (KWW, eq 4) rather than biexponential (eq 2) indicating that the assumed model of diffusion in two different environments, each being characterized by one single tracer diffusivity, is only an approximation. The stretching parameter β that usually is interpreted as representing a distribution of relaxation times due to spatial or dynamic heterogeneities[36] grew from 0.7 to a value of nearly unity with water loss. The decay then turned out to be almost exponential, manifesting conversion of the latex film to a spatially homogeneous state at a crossover concentration of residual water of about 1%, close to its solubility in the polymer.

The diffusion coefficient calculated from the averaged decay time via eq 5 was found to be a function of the grating period (Figure 3) and can thus be interpreted as in our previous work[22] in terms of an apparent diffusion coefficient $D_{app} = D_{app}(\Lambda)$, where the Λ dependence arises as a result of the spatial averaging over two compartments of the inhomogeneous system: the latex cores and the surrounding hydrophilic interface impregnated with water. At the highest water content that allows for FRS measurements (6−7%), the value of D_{app} varies from 7×10^{-17} m^2 s^{-1} at $\Lambda = 180$ nm to 2×10^{-15} m^2 s^{-1} for $\Lambda > 3\ \mu$m. In dry films, $D_{app} = 3 \times 10^{-17}$ m^2 s^{-1} irrespective of the grating distance.

The two-state model provides a fit formula for the dependence of D_{app} on the length scale Λ (eq 6) which allows us to extract the values of the tracer diffusion coefficients $D_{s,f}$ (see Figure 4a) as well as their mean displacements $M_{s,f}$ (Figure 4b) in the two types of spatial domains. The corresponding fits compare very well with the experimental D_{app} values as shown in Figure 3. The complex diffusion behavior of the hydrophobic probe in the drying latex film can now be explained in terms of the property changes of the respective compartments visited by the dye molecules. The features of the particle cores ($D_s = (4 \pm 1) \times 10^{-17}$ m^2 s^{-1}, $M_s = 100 \pm 30$ nm) stayed independent of the water concentration. As in our previous study[22] M_s was found close to the average particle radius. Contrastingly, D_f and M_f decrease significantly as the film dries (Figure 4).

The line shapes of the grating relaxation curves originate from the averaging over two types of heterogeneities. First, there is the averaging over the transport properties of different compartments of the drying film, and second, there may be averaging over a distribution of relaxation times due to local heterogeneities within a given compartment. The first type of heterogeneity is responsible for the grating distance dependence of the apparent diffusion coefficient, $D_{app}(\Lambda)$. Depending on the chosen Λ, tracer diffusion in the "slow" and in the "fast" phase contribute with varying weights to the grating relaxation. The decay at small Λ is predominantly due to dye diffusion in the ("slow") polymer phase, given by D_s, whereas at large Λ the grating is essentially relaxed by dye diffusion in the ("fast") interfacial phase, described by D_f. At intermediate Λ, both types of dye motions contribute, but to varying degrees, thus giving rise to the peculiar length scale dependence $D_{app}(\Lambda)$ depicted in Figure 3.

The spatial heterogeneities within a given compartment are then responsible for the deviation from the biexponential decay curves predicted by the two-state model (cf. eq 2). Clearly, already a distribution of relaxation times in only one compartment would be sufficient to explain the observation of a stretched exponential line shape for the grating relaxation curves in wet latex films.

The results of FRS measurements on diffusion of ACR-540 (hydrophobic tracer) in PBMA latex films are qualitatively very similar to those reported for poly(BMA-*co*-AA).[22] The quantitative difference between the films made of these two polymers is that only about half of the water concentration is needed in PBMA for the

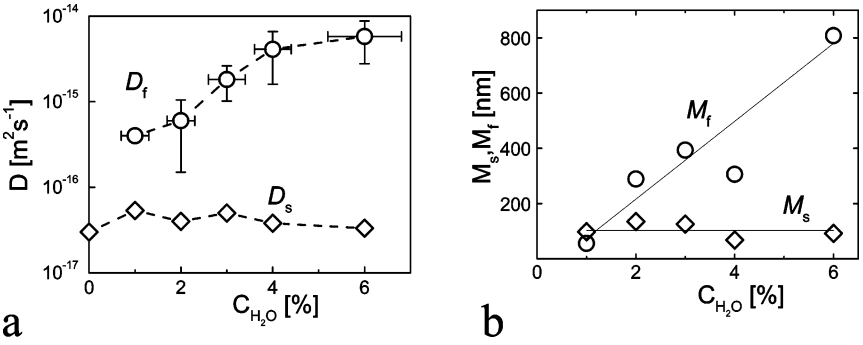

Figure 4. Diffusion coefficients of the hydrophobic tracer in "slow" (D_s) and "fast" (D_f) spatial domains of PBMA latex film (a) and the root-mean-squared diffusive displacements (b) during its residence times in such domains (M_s and M_f, respectively) at 40 °C, as functions of residual water concentration. Lines are guides to the eye.

same effect on tracer diffusion (extent of hydroplasticizing) as in poly(BMA-*co*-AA. This implies that about twice as much water can be absorbed homogeneously into the PBMA-*co*-AA polymer matrix as compared to pure PBMA. This is clearly due to the presence of the AA comonomer. Noticeable is that on drying PBMA becomes transparent (thus making optical measurements possible) at 7% residual water as compared with 18% in poly(BMA-*co*-AA).

The picture of the drying process in latex film that emerges from the analysis of the tracer diffusion data via the two state model is in good agreement with the standard model of film formation:[4] water is lost—besides via water channels that may still be present at water contents as low a 7% (see below)—essentially from the interfacial area, denoted as hydrophilic membranes,[4] while the particle cores remain unaffected as can be seen from their water content independent transport properties (D_s, M_s; cf. Figure 4). This (spatially) heterogeneous drying process continues until the properties of the membranes have approached those of the cores (at water contents depending of the composition of the polymer matrix, e.g. at 1% for pure PBMA). After this the drying proceeds homogeneously from all regions of the latex film until the limiting value of the dry polymer film is reached as can be seen from the disappearance of the Λ dependence of D_{app} in Figure 3. The fate of the hydrophilic membranes on drying can be 2-fold:[4] they can shrink in size but remain intact in the final film or they can break up on drying, thus allowing for particle coalescence via polymer interdiffusion. The former case occurs when the membranes have a cross-linked structure whereas the latter case is typical for membranes consisting of absorbed surfactant molecules as is the case in this work. From SANS experiments,[4] it can be deduced that coalescence occurs in surfactant-stabilized dispersions if the local residual water content has decreased to 5−10%. Even though we do not know the local water content in the probed sample volumes we expect it to differ not to much from the overall residual water content of the whole sample to which our measurements refer. Thus, our experiments probe stages of the drying process where coalescence should be relevant. From rewetting experiments,[37] we could, however, deduce that coalescence was not complete. Exposing fully dried latex films to water, the characteristic length scale dependence of $D_{app}(\Lambda)$ was recovered, but not to full extent. The limiting value $D_{app}(\Lambda \rightarrow \infty)$ for a water-saturated latex film did correspond to a residual water content of about 2−3%. Thus, some parts of the membrane structure have survived the drying process. This is in line with experiments of Joanicot et al.[38] where it was shown that lack of mobility in the cores will block expulsion of hydrophilic membranes, thus keeping parts of the fragmented membranes in place. This indicates that the possibility to probe tracer diffusion in the membranes together with systematic rewetting experiments may be another option to quantitatively monitor coalescence.

Hydrophilic Probe: Empirical Features and Identification of Decay Components. The hydrophilic tracer was employed as a probe complementary to the hydrophobic one. It was supposed to monitor the transport properties of the hydrophilic interface and interstitial water in a similar manner as the hydrophobic tracer probed the polymer phase and the interfacial face. However, the grating relaxation curves show clearly different line shapes in the case of the hydrophilic tracer as compared to latex films with identical water content probed by the hydrophobic dye. In the case of the hydrophilic dye, the shapes of the decay curves (Figure 2, full symbols) clearly demonstrate the presence of two stages of decay. Unlike the decay of gratings based on the hydrophobic dye, the data points cannot be fitted satisfactorily to a single KWW (stretched exponential) function. Instead, a fit by two stretched-exponential terms

$$I(t) = (a_1 \exp(-(t/\tau_1)^{\beta_1}) + a_2 \exp(-(t/\tau_2)^{\beta_2}))^2 \quad (7)$$

was necessary to obtain an acceptable description of the grating relaxation curve.

If one analyzes the grating relaxation curves in a similar manner as in the case of the hydrophobic tracer (see above) there are now two apparent diffusion coefficients $D_i = D_{i.app}(\Lambda) = \Lambda^2/(4\pi^2\langle\tau_i\rangle)$, where $\langle\tau_i\rangle = \beta_i^{-1}\Gamma(\beta_i^{-1})\tau_i$ and $i = 1, 2$, whose physical basis has to be explained. The most simple model would be that a third compartment is involved, which obviously would have to be identified as the polymer phase (D_s) and that the exchange of the dye between the three compartment proceeds consecutively, e.g. $D_s \leftrightarrow D_f \leftrightarrow D_w$. In this case it could be expected that the saturation plateau of an apparent diffusion coefficient would be at the level where another one starts (assuming $D_s \ll D_f \ll D_w$ as appears plausible from consideration of the microviscosities of the corresponding compartments). The Λ dependence of D_1 (triangles) and D_2 (squares) is shown in Figure 5 over a wide range of Λ extending over about 3 decades. The dotted lines, drawn as a guide to the eye, have a more complex shape than those in Figure 3 representing a fit to the two state model for the *hydrophobic* dye diffusion. The results are also not

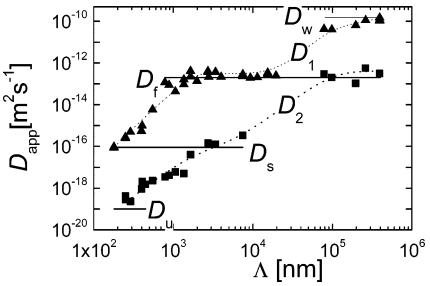

Figure 5. Evaluation of FRS results on diffusion of the hydrophilic tracer in a PBMA latex film with 3% residual water in terms of two apparent diffusion coefficients (▲, D_1; ■, D_2) as obtained from fits with two stretched exponentials (eq 7). The horizontal lines indicate results of a four-component fit (eq 9; see text for further details). The dotted lines are guides to the eye.

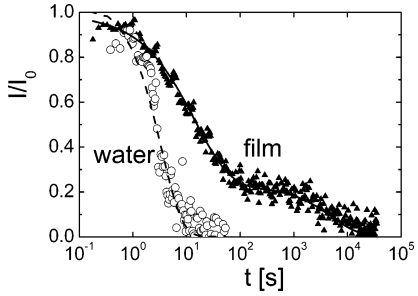

Figure 6. Grating decays due to diffusion of the hydrophilic tracer in bulk water ($D = 6 \times 10^{-10}$ m^2 s^{-1}, circles and dashed line) and wet (3% water) latex film (triangles and solid line) at 40 °C. In the latter case two stages of decay are visible that are interpreted as diffusion in a water phase ($D_w = 3 \times 10^{-11}$ m^2 s^{-1}) and a hydrophilic interface ($D_f = 2 \times 10^{-13}$ m^2 s^{-1}). The spatial period of the grating is 0.4 mm.

consistent with what is to be expected from the consecutive three-state model as already one of the apparent diffusion coefficients (D_1) shows such a two-step Λ dependence. Clearly, the diffusional behavior of the *hydrophilic* dye tracer is more complex and cannot be approximated even by three diffusion coefficients. As discussed further below an interpretation in terms of four diffusivities, D_w, D_f, D_s, and D_u, is possible, and the resulting values are indicated in Figure 5 as horizontal lines.

Water Phase. A possibility to simplify the complex grating relaxation dynamics is to select the grating distance Λ such that only the dye diffusion in two compartments contributes to the signal. To focus on the contribution of the water phase extremely large grating distances (Λ = 0.1−0.4 mm) had to be chosen. The corresponding measurements revealed very fast diffusional decay of the gratings recorded in wet films with the hydrophilic dye, which is followed by an also diffusional slower decay stage. Both processes were confirmed as being diffusional by varying Λ. An example of this type of grating decay in a wet (3% residual water) film is shown in Figure 6, and it is compared with the one-stage decay observed under the same conditions in bulk water. A fit of the two stage decay with the two state model (eqn.2) yields the diffusion coefficients D_w = 3×10^{-11} m^2 s^{-1} and $D_f = 2 \times 10^{-13}$ m^2 s^{-1} which correspond to the upper two horizontal lines in Figure 5. D_w varies from 3×10^{-11} m^2 s^{-1} for 3% to 2×10^{-10} m^2 s^{-1} for 7% residual water. The diffusion coefficient of ACR-hydr, 6×10^{-10} m^2 s^{-1}, measured in bulk water, is noticeably lower than the water self-diffusion coefficient, 3.14×10^{-9} m^2 s^{-1} at 40 °C [39]. It seems plausible to assign the discovered decay stage to the diffusion of tracer molecules in a sort of water channels, whose properties deviate the further from those of bulk water the less water remains in the film. The difference between the diffusion coefficients in the film and in bulk water can be in principle due to an increased viscosity and (or) the tortuosity of the "water channels".[40−42] From viscosity measurements of water containing surfactant in concentrations up to the critical micellar concentration we find no significant effect of the surfactant on self-or tracer diffusion. Thus, it seems that tortuosity is the dominant effect. We have denoted the diffusion coefficient in this compartment by D_w (the subscript "w" stands for water). This water phase stayed "invisible" for the hydrophobic dye, ACR-540, because of its complete insolubility in water. These supposed channels do not disturb the samples' optical clarity. Hence, their thickness must be small in comparison with the light wavelength. However, the remarkable contribution of D_w to the grating decay lets one believe that the channels can be rather long: 20% degradation of the grating with Λ = 0.4 mm corresponds to a root-mean-squared displacement within the water phase as large as $\sqrt{\langle x^2 \rangle} = \sqrt{2Dt} = \sqrt{-\ln 0.8/2} \cdot \Lambda/\pi \approx 0.04$ mm! The dependence of the obtained diffusion coefficients D_w on residual water content in the latex films is depicted in Figure 8.

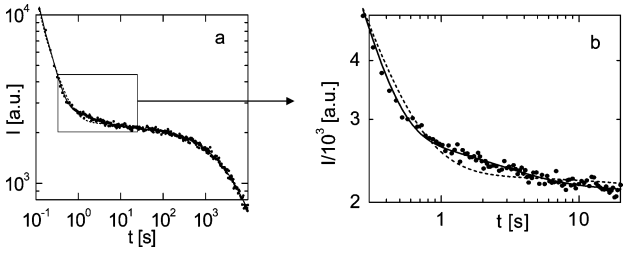

Figure 7. The decay of the grating with spatial period Λ = 2.3 μm, recorded in PBMA latex film (7% residual water) with the hydrophilic tracer (a). The inset in (a) is shown enlarged in (b). Here the weak "slow" (D_s) decay component is best visible (b). The dashed line is the best bi-stretched-exponential fit (eq 7); the solid line represents three-stretched-exponential fit (eq 8).

Particle Cores and Hydrophilic Interface. In Figure 7, a careful analysis of the grating decay is shown for an intermediate grating distance (Λ = 2.3 μm). Here, the fast decay, which is dominant in Figure 6, cannot be observed since it would be in the sub-millisecond time domain ($\tau \propto \Lambda^{-2}$). Thus, the fastest observable decay in Figure 7 corresponds to D_f, the diffusion in the ("fast") interfacial phase attributed to surfactant rich domains. A quantitative analysis (see below) results in D_f values that are considerably larger than those of the hydrophobic dye tracer (see Figure 8). But they are still about 200 times smaller than the D_w values in the water phase.

The data shown in Figure 7 cannot be fitted with a bi-stretched-exponential fit (eq 7) as demonstrated by the dashed line in Figure 7b. Rather a fit with three stretched exponentials had to be employed:

$$I(t) = \left(\sum_{i=1}^{3} a_i \exp(-(t/\tau_i)^{\beta_i})\right)^2 \qquad (8)$$

Thus, an application of the two-state model was not feasible. Instead, the description yields two further

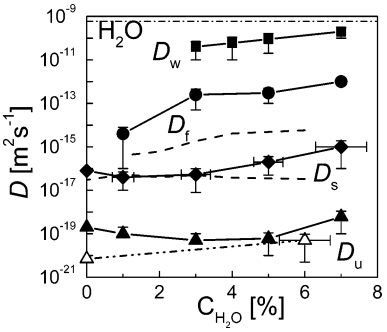

Figure 8. Diffusion coefficients of hydrophilic probes (full symbols, solid lines) as a function of the residual water concentration at 40 °C. The values were obtained by directly fitting the hologram relaxation curve to two or three stretched exponentials as described in the preceding sections. The corresponding data on diffusion of hydrophobic Aberchrome probe (from Figure 4a) are shown in dashed lines labeled D_s and D_f. The dash−dot−dot line and the solid lines are guides to the eye. Key: *dash−dotted line*, diffusion coefficient of the hydrophilic dye in bulk water (6×10^{-10} m^2 s^{-1}); *squares*, water phase of latex film (D_w); *circles*, "fast", hydrophilic interfacial phase (D_f); *diamonds*, "slow" phase associated with particle core domains of PBMA latex films (D_s; *triangles*, effectively immobilized (linked) probes (D_y−"ultraslow"). Full triangles depict the diffusion coefficients of the hydrophilic molecules supposedly captured by surfactant clusters, whereas the open triangles represent diffusion coefficients of polymer chains with photochemically attached phenanthrenequinone molecules.

diffusion coefficients, D_s and D_u, which are discussed further in the text below. Here, we note that $D_s \sim 10^{-16}$ m^2 s^{-1}, corresponding to the intermediate part of Figure 7, agrees rather well with D_s of the hydrophobic dye tracer in the latex particle cores (see Figure 8). However, the "slow" D_s contribution in the grating decay of the hydrophobic tracer is of the order of the volume fraction of the latex particles whereas it amounts to only about 1% in the case of the hydrophilic tracer. Apparently, this is due to the low solubility of the hydrophilic dye in the polymer latex particles.

Bound Probes. An insight as to the nature of the slowest decay component, denoted as D_u (u = ultraslow) can be gained from the comparison of the grating relaxation curve shapes for the hydrophobic and the hydrophilic tracer in dry films (cf. Figure 2). In dry films, the grating decay of the *hydrophobic* tracer was always exponential, implying normal Fickian diffusion in a uniform medium (polymer interior of the latex particles, diffusion coefficient D_s). In the case of the *hydrophilic* dye an additional, slower decay stage was found even if the film was dried over a long period of time. In wet films, this very slow decay stage is present as well. There it follows the stage attributed to the diffusion in polymer (D_s) (Figure 7). It could be monitored within a reasonable duration of the experiment only in the case of small grating distances, especially reflection gratings. For larger Λ only a seemingly permanent coherent background signal was detected instead which can be considered as evidence for diffusional nature of the process.

The decay rate can be characterized by a diffusion coefficient $D_u = 10^{-19}-10^{-18}$ m^2 s^{-1}. The values, which are included in Figure 8 are much lower than any possible diffusion coefficient of a free molecule and are almost as low as that of polymer chains in wet PBMA latex films. Polymer diffusion coefficients $D_{polymer} = 10^{-20}-10^{-19}$ m^2 s^{-1} were obtained in grating relaxation experiments with phenanthrenequinone, a dye which photochemically attaches to polymer chains. The corresponding $D_{polymer}$ values are included in Figure 8 (open triangles). A possible interpretation of the "ultraslow" diffusing fraction of the hydrophilic tracer molecules is to consider them as effectively immobilized, probably associated with surfactant molecules. The existence of such aggregates has been discussed in the context of EPR tracer experiments on latex films.[19−21] However, we have no information on the size of the moving units. The hypothesis that surfactant molecules are involved is supported by the following observation: The slowest diffusion stage (D_u) was found to vanish after long (months) annealing of dry films under ambient conditions which can be explained by the well-known exudation,[13,14] i.e., the spatial segregation of the surfactant and its concomitant enrichment at the polymer−air or the polymer−substrate interface; only the normal diffusion in the bulk polymer (D_s) persisted in the end.

The two grating distance dependent apparent diffusion coefficients (Figure 5) found in our experiments can now be explained as resulting from a superposition of the four diffusion processes discussed above, whose diffusion coefficients are shown in Figure 5 as horizontal lines. Their apparent contributions depend on whether the respective decay times (which depend on the grating distance as Λ^2) correspond to the time window of the experiment. In a regime of large spatial periods, the residual slowly decaying grating appears weaker than the fast component. In addition, this residual weak grating looks permanent within the experimental time scale and may be easily confused with the background noise. On the other hand, at a smaller grating distance (high spatial frequency, especially in reflection geometry) the fast decay stage escapes to the microsecond time range inaccessible to the experimental setup. In Figure 5, the intermediate plateau value of the mixed process D_1 ($\Lambda = 1-10\ \mu$m) and the upper plateau value of D_2 ($\Lambda > 100\ \mu$m) at about 2×10^{-13} m^2 s^{-1} correspond to the same process with a single diffusion coefficient (D_f).

Master Curve. The difference between the diffusion coefficients corresponding to the fastest and the slowest stages of grating decay amounts to as much as 9 decades. Therefore, the whole decay cannot be monitored within any single course of measurement at one grating distance. As the rates of the diffusion processes are proportional to the squared grating period, $\langle\tau_i\rangle^{-1} = 4\pi^2 D_i/\Lambda^2$, the latter can be used as a scaling factor for the kinetic curves. Summarizing the results of the decay measurements at different spatial periods Λ, we can build a master curve with four distinct stages by plotting the data obtained from the experiments vs a renormalized time: $4\pi^2\Lambda^{-2}\cdot t$. The example of the latex film with 7% residual water is presented in Figure 9. It should be noted that the huge range of rescaled time extending over 10 decades was only possible because of the large time *and* Λ ranges accessible with our optical setup (see above). The description of the complete decay requires a four-component fit formula:

$$I(t) = \left(\sum_{i=1}^{4} a_i \exp(-(t/\tau_i)^{\beta_i})\right)^2 = (a_w \exp(-(t/\tau_w)^{\beta_w}) + a_f \exp(-(t/\tau_f)^{\beta_f}) + a_s \exp(-(t/\tau_s)^{\beta_s}) + a_u \exp(-(t/\tau_u)^{\beta_u}))^2 \quad (9)$$

In the given case of 7% residual water, the four processes can be described by the diffusion coefficients:

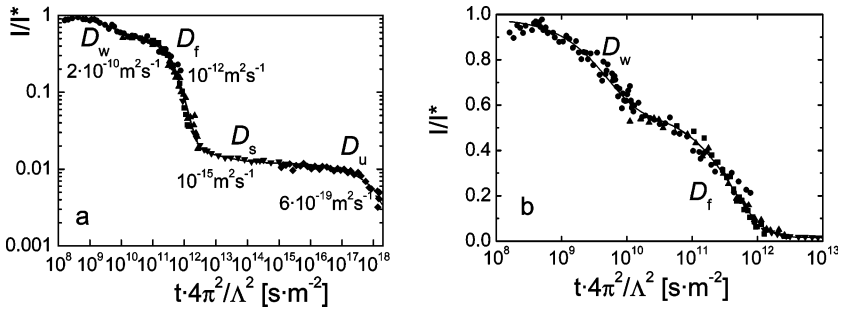

Figure 9. Decay of photoinduced grating in PBMA latex film with the hydrophilic dye and 7% residual water. Master plot for the gratings with different spatial periods, Λ: 0.4, 2.3, 7.7, 22, and 285 μm. In a logarithmic scale (a), four distinct stages of decay are distinguishable caused by dye diffusion in water channels (D_w), in hydroplasticized interface layer (D_f), in particle cores (D_s), and captured in "surfactant clusters" (see text) (D_u). In a linear intensity scale (b), only the two first stages can be seen: D_w and D_f. The contributions of the two others appear negligible. The solid line is the best fit in accordance with a squared four-stretched exponential decay (eq 9) with fractional contributions of the stages given by $a_w = 0.23$, $a_f = 0.64$, $a_s = 0.02$, and $a_u = 0.11$, respectively. For clarity, the number of experimental points is reduced by a factor of ∼10 in the figure.

$D_w = 2 \times 10^{-10}$ m^2 s^{-1}, $D_f = 1.1 \times 10^{-12}$ m^2 s^{-1}, $D_s = 10^{-15}$ m^2 s^{-1}, $D_u = 6 \times 10^{-19}$ m^2 s^{-1}, with relative contributions to the grating modulation a_w:a_f:a_s:a_u = 0.23:0.64:0.02:0.11. The grating decay in wet latex films is mainly due to the two fastest processes that occur in water-containing environments, as shown in the log−log plot of Figure 9a. If a linear signal intensity scale is chosen (Figure 9b), only these two fast decay stages are visible. The first process results in the diffracted intensity decay to $(1 - a_w/(a_w + a_f + a_s + a_u))^2 = 0.6$ of its initial value, almost all the rest (0.38) is due to the second process, and only the last fraction, $(1 - (a_w + a_f)/(a_w + a_f + a_s + a_u))^2 = 0.02$, of the intensity decays due to the two slowest processes. The two main first (fast) decay stages are exponential ($\beta = 1$). The two slower decays are significantly stretched ($\beta_s = 0.5$ and $\beta_u = 0.6$) probably because of spatial heterogeneity.

The fitting of the hologram relaxation master curves in terms of stretched exponentials is in the first place nothing more than a convenient operational parametrization of experimental data in order to check for the number of dynamic processes necessary to get a satisfactory description of the complex dynamics of the hydrophilic tracer. At first sight, a four-component fit with the concomitant number of adjustable parameters may seem to be of questionable validity. However, one should keep in mind that the fits were applied to a very broad database—master plots spanning 10 orders of magnitude in time and composed of typically five grating distances with about 200 data points per decay curve. As can be seen from the master plot, Figure 9a, three well-separated decay steps are very clearly visible. Whereas the first two were exponential, the final decay was strongly stretched beyond any doubt. The only ambiguity that remains is the description of that part of the relaxation curve marked by D_s. Here, no clear relaxation step can be identified and only the failure to fit the corresponding part of the line shape by the superposition of even two stretched exponentials (cf. Figure 7) indicates the presence of an additional dynamic component. The nature of this process—diffusional, relaxational, or other—could not unambiguously clarified as the corresponding part of the decay curve could as well have been described by a log(t) behavior. Lacking a theoretical frame and given the very small contribution of this process, the application of a fourth stretched exponential seemed to be the most simple approach. The most probable error introduced by this representation is an overestimation of the stretching at longer times (i.e., an underestimation of the β values of the process denoted as D_u), which will translate into a corresponding error of the related diffusion coefficients. The overall qualitative picture as summarized in Figure 8 will, however, not be affected.

The presence of four relaxation components indicates that the analysis of the grating relaxation dynamics would require the extension of the two-state model analysis used in the case of the *hydrophobic* tracer diffusion data to a four-state model in the case of the *hydrophilic* dye. Such an extension would imply the diagonalization of a system of four coupled Fickian diffusion equations with exchange terms between each type of compartments, leading to an extension of eq 2 to a sum of four exponentials. In this representation one would recover eq 9 with $\beta_i = 1$, the a_i would be identified as the effective volume fractions p_i' and from the relaxation times one would recover effective diffusion constants D'_i, which would then depend in a manner analogous to, but more complicated than, eq 3 on the properties of the compartments. Such an extension is, however, beyond the scope of the present work. In principle, the applicability of a reduced description could then be checked, i.e., allowing exchange only between certain compartments. The fact that the Λ^{-2} scaling of Figure 9 can be approximated by a master curve for data taken at different Λ, however, implies that Fickian diffusion occurs in the corresponding spatial domains with the exchange between compartments being rather small. This indicates that the lifetimes of the dye tracer molecules in the respective domains should be longer than $\langle\tau_i\rangle = \tau_i = \Lambda^2/4\pi^2 D_i$) for the largest Λ where the Λ^{-2} dependence could be checked. In this case the effective diffusion constants D'_i would reduce to the true diffusion coefficients D_i. However, a careful scrutiny of the master plots indicates that the Λ^{-2} scaling is not perfectly fulfilled, deviations being most pronounced in the transition region between the processes denoted as D_f and D_s. Thus, the description of the master plot data in terms of four diffusion coefficients D_w, D_f, D_s, and D_u has to be considered as a first approximation. It has, therefore, to be kept in mind that these diffusion coefficients are effective diffusion coefficients just like D_s' and D_f' in the two-state model and may contain contributions (small as they may be) from other than the designated compartments (cf. eqs 2 and 3). Nevertheless, these effective diffusion coefficients can be used as operational model parameters, which allow one to quantitatively describe the diffusion of small hydrophilic

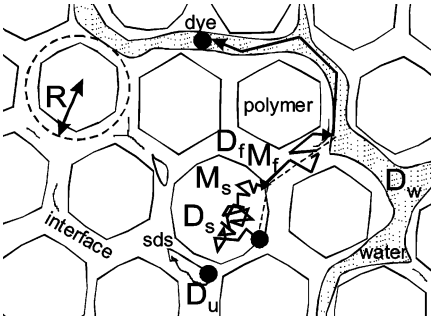

Figure 10. Four possible locations of the hydrophilic tracer in wet latex film, as revealed by grating relaxation experiments: (1) water channels (diffusion coefficient D_w); (2) hydroplasticized hydrophilic interface between the latex particles—"fast" domain (diffusion coefficient D_f, root-mean-squared displacement M_f); (3) polymer interior of latex particles—"slow" domain (D_s, M_s); (4) (supposedly) surfactant clusters; the dye molecule is captured and only can move by "ultraslow" diffusion with the aggregate (diffusion coefficient D_u).

molecules in drying latex films with the aim to compare different latex materials or varying drying conditions.

In Figure 10, we show a schematic drawing of diffusion in the four different environments that seem to be accessible by the hydrophilic dye tracer.

Contrastingly, the hydrophobic tracer can only be situated in two of these domains: the interface and the particle cores (f, s).

Conclusion

Forced Rayleigh scattering (holographic grating decay) experiments in latex films with the *hydrophobic* photochromic fulgide dye tracer Aberchrome-540 make it possible to study its diffusion in the polymer cores of latex particles and in the hydrophilic interfacial regions surrounding the particles. Efficient exchange between the domains leads to spatial averaging of the apparent diffusion coefficient with the weight fractions depending on the spatial scale (ratio of particle size and grating period) and the dye affinity to the environment. The diffusion is significantly enhanced in the hydroplasticized interface, but the major contribution to the grating decay is due to slower diffusion in the particle cores.

The modified *hydrophilic* fulgide dye, ACR-hydr (see formula **II** in experimental part) is a suitable selective FRS probe for the "wet" compartment. In this case, *four* stages of grating decay are visible in the decay curves. Although there is no unique way of analyzing these complex decays we have chosen a fit with four stretched exponentials, which results in a plausible interpretation consistent with all available information. The respective diffusion coefficients extend over a wide range of 9 decades (see Figures 5, 8, and 9). The two fast processes, responsible for the major part of the grating decay, occur in water-rich areas. Supposedly continuous water channels for the fastest part correspond to a tracer diffusion coefficient close to that in bulk water. The second part corresponds to the hydrophilic interface between the latex particles. A few percent of the dye diffuse slowly in the particle cores; the rest are nearly immobilized being supposedly captured by surfactant clusters. The water-containing domains undergo dramatic changes and finally collapse as the film dries; they reveal different features to the two probes with different hydrophilicities. The interior of the latex particles does not change much in the drying process and apparently looks similar to the hydrophobic and hydrophilic dyes.

A combination of experiments using two efficient dyes with similar photochemical properties, molecular shape, and volume but significantly different hydrophilicity provides an instrument for complementary description of a spatially inhomogeneous medium with hydrophobic and hydrophilic regions. An application of this approach in order to elucidate the role and the fate of surfactant molecules in drying latex films, to model the behavior of small molecular additives in latex films as well as an extension to more complex structured core shell latex films appears very promising and will be pursued in future work.

Acknowledgment. Financial support by the Deutsche Forschungsgemeinschaft (Grant 436 RUS 17/47/01) and the Bumdesministerium für Bildung und Forschung (BMBF), Grant 03D0060A5, is gratefully acknowledged. We thank Petra Wetzel for measurements of the viscosity of SDS solutions.

References and Notes

(1) Steward, P. A.; Hearn, J.; Wilkinson, M. C. *Adv. Colloid Interface Sci.* **2000**, *86*, 195.
(2) Winnik, M. A. In *Emulsion Polymerization and Emulsion Polymers*; Lovell, P. A., El-Aasser, M. S., Eds.; Wiley: New York, 1997; p 467.
(3) Keddie, J. L. *Mater. Sci. Eng.* **1997**, *21*, 101.
(4) Chevalier, Y.; Pichot, C.; Graillat, C.; Joanicot, M.; Wong, K.; Maquet, J.; Lindner, P.; Cabane, B. *Colloid Polym. Sci.* **1992**, *270*, 806.
(5) Chevalier, Y. *Trends Polym. Sci.* **1996**, *4*, 197.
(6) Dingenouts, N.; Ballauff, M. *Langmuir* **1999**, *15*, 3283.
(7) Wang, Y.; Winnik, M. A. *J. Phys. Chem.* **1993**, *97*, 2507.
(8) Kim, H.-B.; Winnik, M. A. *Macromolecules* **1995**, *28*, 2033.
(9) Feng, J.; Winnik, M. A. *Macromolecules* **1997**, *30*, 4324.
(10) Feng, J.; Pham, H.; Stoeva, V.; Winnik, M. A. *J. Polym. Sci., Part B: Polym. Phys.* **1998**, *36*, 1129.
(11) Juhué, D.; Lang, J. *Langmuir* **1993**, *9*, 792.
(12) Butt, H.-J.; Kuropka, R.; Christensen, B. *Colloid Polym. Sci.* **1994**, *272*, 1218.
(13) Juhué, D.; Wang, Y. C.; Lang, J.; Leung, O. M.; Goh, M. C.; Winnik, M. A. *J. Polym. Sci., Part B: Polym. Phys.* **1995**, *33*, 1123.
(14) Du Chesne, A.; Gerharz, B.; Lieser, G. *Polym. Int.* **1997**, *43*, 187.
(15) Joanicot, M.; Wong, K.; Maquet, J.; Chevalier, Y.; Pichot, C.; Graillat, C.; Lindner, P.; Rios, L.; Cabane, B. *Prog. Colloid Polym. Sci.* **1990**, *81*, 175.
(16) Holl, Y. *Macromol. Symp.* **2000**, *151*, 473.
(17) Baumgart, T.; Cramer, S.; Jahr, T.; Veniaminov, A.; Adams, J.; Fuhrmann, J.; Jeschke, G.; Wiesner, U.; Spiess, H. W.; Bartsch, E.; Sillescu, H. *Macromol. Symp.* **2000**, *151*, 451.
(18) Bartsch, E.; Jahr, T.; Veniaminov, A.; Sillescu, H. *J. Phys. IV Fr.* **2000**, *10*, 289.
(19) Cramer, S. E.; Bauer, C.; Jeschke, G.; Spiess, H. W. *Appl. Magn. Reson.* **2001**, *21*, 495.
(20) Cramer, S. E.; Jeschke, G.; Spiess, H. W. *Macromol. Chem. Phys.* **2002**, *203*, 182.
(21) Cramer, S. E.; Jeschke, G.; Spiess, H. W. *Macromol. Chem. Phys.* **2002**, *203*, 192.
(22) Veniaminov, A.; Jahr, T.; Sillescu, H.; Bartsch, E. *Macromolecules* **2002**, *35*, 808.
(23) Yokoyama, Y. *Chem. Rev.* **2000**, *100*, 1717.
(24) Kardinahl, T.; Franke, H. *Appl. Phys. A: Mater. Sci. Process.* **1995**, *61*, 23.
(25) Heuberger, G.; Sillescu, H. *J. Phys. Chem.* **1996**, *100*, 15255.
(26) Veniaminov, A. V.; Sillescu, H. *Chem. Phys. Lett.* **1999**, *303*, 499.
(27) Uhlmann, E.; Gauglitz, G. *J. Photochem. Photobiol. A—Chem.* **1996**, *98*, 45.
(28) Kanetakis, J.; Sillescu, H. *Chem. Phys. Lett.* **1996**, *252*, 127.
(29) Veniaminov, A. V.; Sillescu, H. *Macromolecules* **1999**, *32*, 1828.
(30) Balinov, B.; Linse, P.; Sonderman, O. *J. Colloid Interface Sci.* **1996**, *182*, 539.

(31) Zimmerman, J. R.; Brittin, W. E. *J. Phys. Chem.* **1957**, *61*, 1328.
(32) Kärger, J.; Pfeifer, H.; Heink, W. *Adv. Magn. Reson.* **1988**, *12*, 1.
(33) Kärger, J. *Ann. Phys. (Leipzig)* **1969**, *24*, 1.
(34) Hurd, C. D.; Wilkinson, K. *J. Am. Chem. Soc.* **1948**, *70*, 739.
(35) Darsy, P. J.; Heller, H. G.; Strydom, P. J.; Whittall, J. *J. Chem. Soc., Perkin Trans. 1* **1981**, 202.
(36) Sillescu, H. *J. Non-Cryst. Solids* **1999**, *243*, 81.
(37) Bartsch, E.; Jahr, T.; Eckert, T.; Sillescu, H.; Veniaminov, A. *Macromol. Symp.* **2003**, *191*, 151.
(38) Joanicot, M.; Wong, K.; Richard, J.; Maquet, J.; Cabane, B. *Macromolecules* **1993**, *26*, 3168.
(39) Simpson, J. H.; Carr, H. Y. *Phys. Rev.* **1958**, *111*, 1201.
(40) Chan, W.; Pershan, P. S. *Phys. Rev. Lett.* **1977**, *39*, 1368.
(41) Rottstegge, J.; Landfester, K.; Wilhelm, M.; Spiess, H. W.; Heldmann, C. *Colloid Polym. Sci.* **2000**, *278*, 236.
(42) Bhattacharyya, K.; Bagchi, B. *J. Phys. Chem. A* **2000**, *104*, 10603.

MA0258962